



**HAL**  
open science

# Modeling the Onset of Earthquake-Triggered Landslides on Slip Surfaces Governed by Rate-And-State Friction

H. Lestrelin, J P Ampuero, E. Diego Mercerat, Françoise Courboux

► **To cite this version:**

H. Lestrelin, J P Ampuero, E. Diego Mercerat, Françoise Courboux. Modeling the Onset of Earthquake-Triggered Landslides on Slip Surfaces Governed by Rate-And-State Friction. *Geophysical Research Letters*, 2024, 51 (24), pp.e2024GL110695. 10.1029/2024gl110695 . hal-04861810

**HAL Id: hal-04861810**

**<https://hal.science/hal-04861810v1>**

Submitted on 2 Jan 2025

**HAL** is a multi-disciplinary open access archive for the deposit and dissemination of scientific research documents, whether they are published or not. The documents may come from teaching and research institutions in France or abroad, or from public or private research centers.

L'archive ouverte pluridisciplinaire **HAL**, est destinée au dépôt et à la diffusion de documents scientifiques de niveau recherche, publiés ou non, émanant des établissements d'enseignement et de recherche français ou étrangers, des laboratoires publics ou privés.



Distributed under a Creative Commons Attribution 4.0 International License

# Geophysical Research Letters®

## RESEARCH LETTER

10.1029/2024GL110695

## Modeling the Onset of Earthquake-Triggered Landslides on Slip Surfaces Governed by Rate-And-State Friction



### Key Points:

- Numerical and analytical modeling of earthquake-induced landslides on slip surfaces governed by rate-and-state friction
- The frictional state variable tracks the landslide fatigue manifested by progressive weakening of the slip surface
- Landslide triggering by low- and high-frequency shaking is controlled by peak acceleration and velocity, respectively

### Supporting Information:

Supporting Information may be found in the online version of this article.

### Correspondence to:

H. Lestrelin,  
[hugo.lestrelin@hotmail.com](mailto:hugo.lestrelin@hotmail.com)

### Citation:

Lestrelin, H., Ampuero, J. P., Mercerat, E. D., & Courboux, F. (2024). Modeling the onset of earthquake-triggered landslides on slip surfaces governed by rate-and-state friction. *Geophysical Research Letters*, 51, e2024GL110695. <https://doi.org/10.1029/2024GL110695>

Received 7 JUN 2024

Accepted 4 OCT 2024

### Author Contributions:

**Conceptualization:** H. Lestrelin, J. P. Ampuero, E. D. Mercerat, F. Courboux

**Investigation:** H. Lestrelin

**Methodology:** H. Lestrelin,

J. P. Ampuero, E. D. Mercerat,

F. Courboux

**Software:** J. P. Ampuero

**Supervision:** J. P. Ampuero,




E. D. Mercerat, F. Courboux

**Writing – original draft:** H. Lestrelin

**Writing – review & editing:** H. Lestrelin,

J. P. Ampuero, E. D. Mercerat,

F. Courboux

H. Lestrelin<sup>1,2</sup> , J. P. Ampuero<sup>2</sup> , E. D. Mercerat<sup>1,2</sup>, and F. Courboux<sup>2</sup> 

<sup>1</sup>CEREMA, Sophia-Antipolis, Valbonne, France, <sup>2</sup>Observatoire de la Côte d'Azur, IRD, CNRS, Géoazur, Université Côte d'Azur, Valbonne, France

**Abstract** Earthquake-triggered landslides are a severe hazard and contribute to landscape evolution. To understand their process and controlling factors, we model the onset of seismically-triggered slip on pre-existing slip surfaces governed by laboratory-based rate-and-state friction, including wave propagation effects. Through numerical simulations and theoretical analysis, we identify how friction properties, landslide thickness and incident wave attributes (frequency, duration, amplitude) control slope stability. We find that the frictional state variable tracks the cyclic fatigue of the slip surface, its progressive weakening with each wave cycle. Wave propagation effects introduce two regimes depending on frequency relative to the two-way travel time across the landslide thickness: the stability criterion is well approximated by a threshold on incident peak acceleration at low frequencies, and on peak velocity at high frequencies. We derive analytical approximations, validated by simulations, suitable to apply the model to evaluate landslide stability under arbitrary input motions.

**Plain Language Summary** Landslides induced by earthquake shaking cause human and economic losses. Understanding their triggering mechanism is a key to reduce their impact. Here we propose a new model for the onset of seismically-triggered landslide slip using a friction law based on laboratory experiments. Studying the model mathematically and through computer simulations, we identify the specific attributes of the landslide and incident seismic waves that control slope stability. We find that the decrease of the frictional state variable is a good proxy for the approach to instability. The landslide triggering criterion is well described by a peak acceleration threshold if the landslide is shallow or the earthquake shaking is dominated by low frequencies, and by a peak velocity threshold for deep landslides or high-frequency shaking. Finally, we develop equations that can be used to assess landslide stability to shaking without the need for computer simulations.

## 1. Introduction

Seismically-triggered landslides contribute to casualties and economic losses during earthquakes (Bird & Bommer, 2004; Keefer, 1984; Tang et al., 2011; Wang et al., 2014). They are also a key component of long-term continental mass balance leading to interactions between tectonics and landscape evolution. Submarine landslides can cause damaging tsunamis and provide useful constraints for paleo-seismology (e.g., Clare et al., 2020; Goldfinger et al., 2012; Gombert, 2018). A current open question is which ground motion parameters are the best predictors of landslide triggering (Dahal et al., 2023). To be scalable, hazard assessment in practice requires simplified approaches involving synoptic parameters to describe the input ground motions. Parameters considered include Peak Ground Acceleration (PGA), Peak Ground Velocity (PGV), frequency content, duration. It has become evident that no single parameter works universally. Here we address this question through a physics-based model that includes the interactions between two important factors: friction evolution and wave propagation.

Various methods have been proposed to model seismically-triggered landslides. Common approaches are the pseudo-static and Newmark methods (e.g., Chousianitis et al., 2014; Djukem et al., 2024; Kramer & Smith, 1997; Newmark, 1965). Those analyses are straightforward but generally assume a constant friction coefficient and a rigid sliding block and ignore wave propagation across the landslide thickness. More advanced models have been developed, such as the stress-deformation analysis (Jibson, 2011) or models encompassing the formation and growth of the slip surface (Puzrin et al., 2010), but require more parameters and are therefore more complex to apply. Advanced friction laws motivated by laboratory experiments have also been included in landslide models (Chau, 1995; Viesca & Rice, 2012), in particular for re-activated landslides with a pre-existing slip surface. Various observations suggest that the frictional behavior of landslide basal sliding surfaces can be modeled with

© 2024. The Author(s).

This is an open access article under the terms of the [Creative Commons Attribution License](https://creativecommons.org/licenses/by/4.0/), which permits use, distribution and reproduction in any medium, provided the original work is properly cited.



The sign of  $a - b$  determines the stability of sliding in the absence of external triggering loads: if  $a > b$ , friction increases with slip velocity at steady state (velocity-strengthening) and thus slip tends to be stable; if  $a < b$  (velocity-weakening) slip can be unstable.

Although our model applies to arbitrary incident waveforms, we illustrate the model response by considering monochromatic incident waves modulated by a Gaussian envelope:

$$V_{inc}(t) = \bar{V} e^{-\frac{1}{2} \left( \frac{10(t-T/2)}{T} \right)^2} \sin(2\pi f_{inc}(t - T/2)) \quad (4)$$

where  $\bar{V}$  is the peak amplitude,  $T$  the characteristic duration and  $f_{inc}$  the frequency of the wave. Equating the shear stress and frictional strength on the slip surface:

$$\tau_0 + \tau_{inc} + \tau_{ref} + \tau_{slip} = f(V, \theta) \sigma_0 \quad (5)$$

On the left hand side, the shear stress involves the initial shear stress  $\tau_0$  and the dynamic contributions by the incident seismic wave,  $\tau_{inc}$ , by its reflection at the free surface,  $\tau_{ref}$ , and by slip,  $\tau_{slip}$ . The latter is given by (Text S1 in Supporting Information S1):

$$\tau_{slip}(t) = -\frac{\mu}{2C_s} V(t) + \frac{\mu}{2C_s} V(t - \Delta T) \quad (6)$$

where  $\Delta T = 2h/C_s$  is the two-way travel time across the landslide thickness. The first term is the radiation damping induced by waves leaving the slip surface in the normal direction. The second term is the delayed stress carried by the slip-induced waves reflected at the free surface.

We set model parameter values representative of general geological landslide properties for example, (Kelner et al., 2016; Shanmugam & Wang, 2015; Sultan et al., 2004) and friction experiments on landslide materials (Agliardi et al., 2020; Handwerker et al., 2016; Helmstetter et al., 2001; Kang et al., 2022; Skempton, 1985), reported in Table S1 in Supporting Information S1. We simulate seismic wave propagation and induced slip using the spectral element method (Ampuero et al., 2002; Kaneko et al., 2008) implemented in the software sem2dpack (Ampuero et al., 2024). We apply periodicity conditions on the side boundaries, absorbing conditions on the bottom boundary and a free surface condition on the top boundary.

### 3. Results

#### 3.1. Instability and Landslide Fatigue

For a given frequency and duration of the incident wave, unstable slip (a landslide) is triggered if the incident wave amplitude is large enough. We illustrate the difference between stable and unstable triggered slip by comparing two simulations with slightly different incident wave amplitudes (Figure 2). The two cases have  $h = 14$  m,  $a < b$ . The incident waves have peak velocities  $\bar{V}$  of 0.4 m/s (red) and 0.47 m/s (blue), respectively, duration  $T = 60$  s comparable to that of seismic shaking from a large earthquake, and frequency  $f_{inc} = 0.5$  Hz. The triggered slip (dashed curves in Figure 2a) is stable and remains limited in the first case ( $\sim 0.1$  mm) but is unstable and reaches large values in the second case ( $> 1$  m). In both cases, the slip history features multiple steps following each peak of the incident wave velocity (solid lines in Figure 2a). The slip steps are larger for the stronger incident wave case.

The evolution of the state variable  $\theta$  indicates the proximity to instability and provides a proxy of landslide fatigue. Like slip,  $\theta$  also features a step-like evolution (solid curves in Figure 2b): it drops sharply with each peak of the incident wave, weakening the slip surface in a process akin to cyclic fatigue. The transition to unstable slip, manifested by very high slip rates (dashed curves in Figure 2b), happens only if and when  $\theta/\theta_0$  drops down to almost 0. The amplitude of the steps is highly sensitive to the incident wave amplitude: a 20% increase of  $\bar{V}$  leads to 5 times larger  $\theta$  step drops. Instabilities might require multiple wave cycles, thus landslide stability depends on the duration of shaking (number of cycles).

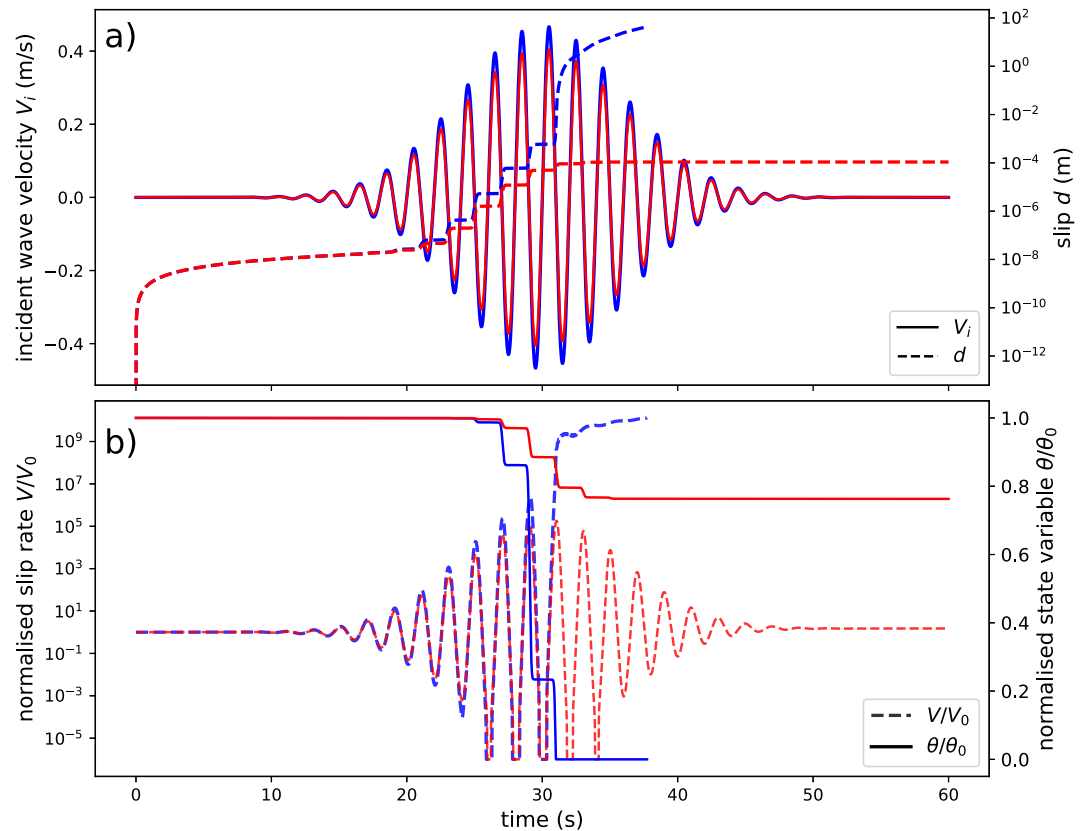


**Figure 2.** Two landslide triggering simulations with slightly different incident wave amplitudes lead to very different outcomes: stable slip (red) and unstable slip (blue). (a) Incident wave velocities (solid lines, their amplitude difference is less than 20%) and triggered slip (dashed lines, their final values differ by six orders of magnitude). (b) Slip velocity (dashed lines) and state variable (solid lines) normalized by their initial values.

Fatigue can accumulate over time scales longer than shaking from a single earthquake. For instance, the case that remained stable during a single earthquake in Figure 2b is triggered by a second identical event about a minute later in the simulation shown in Figure 3. At time scales longer than those considered in this work, we expect fatigue to compete with processes that re-strengthen the slip surface, such as frictional healing (which tends to increase  $\theta$ ) and pore fluid pressure diffusion.

### 3.2. Effect of Landslide Thickness and Frequency Content of the Incident Wave

To characterize systematically the behavior of the model, we conducted parametric studies of slip stability as a function of frequency and amplitude of the incident wave, landslide thickness and frictional properties. We described the incident wave amplitude by the PGA, a parameter commonly used in landslide stability studies for example, (Meunier et al., 2007). We quantified the stability in each simulation by the lowest value of  $\theta/\theta_0$  achieved.

Starting from the cases shown in Figure 2, we ran a set of simulations varying the amplitude and frequency of the incident wave across a relevant range of values. We summarize the results by a stability diagram as a function of PGA and  $f_{inc}$  (Figure 4a). A stability boundary separates stable (red) from unstable (blue) conditions. The boundary is quite sharp, but not infinitely so: over a certain range of conditions close to instability, low values of  $\theta/\theta_0$  are reached without achieving failure. At low frequencies, the stability boundary approaches a PGA threshold (its shape tends to vertical in the diagram). At increasing frequencies, stability is enhanced: a larger PGA is required to trigger a landslide.

To examine the effect of landslide thickness, we conducted a similar set of simulations with a thicker  $h$  of 40 m (Figure 4b). We find that stability is enhanced by increasing  $h$ : slip is stable over a wider range of frequencies and

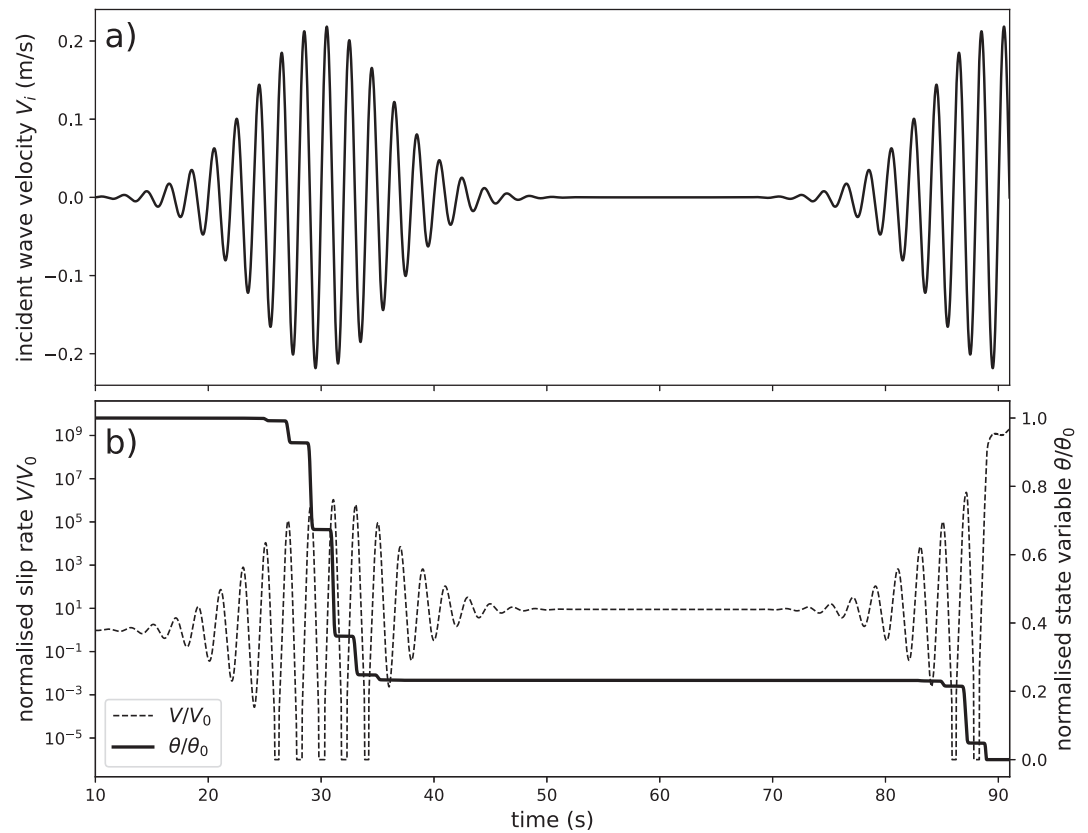


**Figure 3.** Landslide fatigue leads to triggering by a sequence of earthquakes. (a) Incident wave velocity composed of two identical wave packets, 1 min apart. (b) Slip velocity (dashed lines) and state variable (solid lines) normalized by their initial values. Slip surface fatigue can be tracked by the step-wise reduction of  $\theta/\theta_0$  with each wave cycle. Instability, manifested by large  $V/V_0$  values, occurs at  $t \approx 90$  s when  $\theta/\theta_0 \approx 0$ .

amplitudes. At low frequencies (below 1 Hz), the stability boundary is again well described by a PGA threshold. At frequencies around 3.5 Hz, we find stable slip at all values of PGA (a horizontal red corridor in the diagram). The frequency of this strong stability band is the inverse of the two-way travel time  $\Delta T$ . Thus, it arises from the destructive interference between upgoing and downgoing waves. At even higher frequencies, we find a second unstable domain, requiring higher PGA values.

We repeated the parametric studies but on a velocity-strengthening slip surface, with  $a = 0.015 > b = 0.01$  (Figures 4c and 4d). We find that, despite the nominal stability of velocity-strengthening surfaces, they are susceptible to dynamic triggering across a range of incident amplitudes and frequencies comparable to those in the velocity-weakening cases. As expected, for a given frequency, triggering a velocity-strengthening landslide requires higher PGA values.

### 3.3. Insights From Theoretical Analysis

To gain insight on the key parameters controlling slip stability in our model, we developed linear and non-linear theoretical analyses of the landslide response to perturbations. Both of these analysis are fully detailed in Text S1 and S2 in Supporting Information S1. The linear analysis considers small perturbations around the initial steady state due to the incident wave. It yields a closed-form expression that predicts qualitatively the shape of the stability boundaries in Figure 4, up to a multiplicative factor on the PGA. The non-linear analysis considers finite perturbations well above steady state. It provides a closed-form expression of the multiplicative factor. Their combination yields a prediction of the stability boundary that matches quantitatively our simulation results (yellow dashed curves in Figure 4).



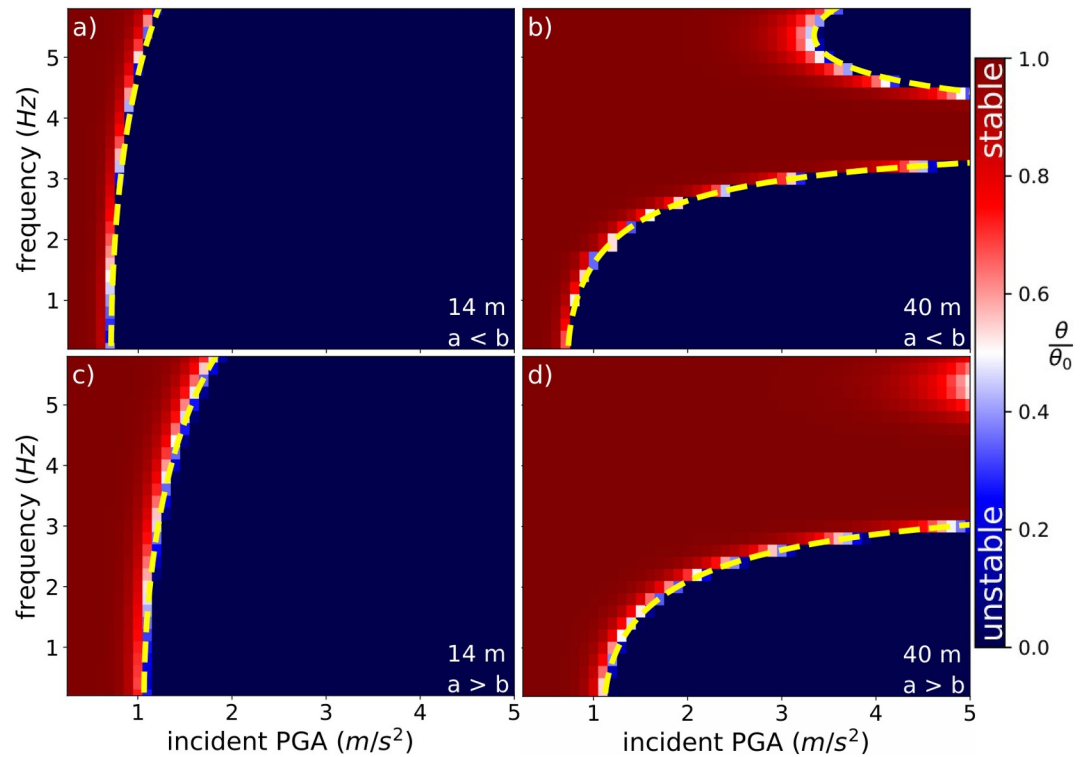


**Figure 4.** Landslide triggering conditions as a function of incident wave frequency and amplitude (Peak Ground Acceleration). Two slip surface depths are considered, 14 m (in a and c) and 40 m (in b and d), and two frictional behaviors, velocity-weakening (in a and b) and velocity-strengthening (in c and d). Other landslide properties are defined in Table S1 in Supporting Information S1. Slip stability is quantified by the normalized state variable: unstable slip corresponds to  $\theta/\theta_0 \approx 0$ . The yellow dashed curve is the stability boundary predicted by the approximate Equation S48 in Text S2 in Supporting Information S1.

The theoretical results enable a more general understanding of the problem, summarized by the stability boundary in non-dimensional form shown in Figure 5. At frequencies lower than  $1/(\pi\Delta T) = C_s/(2\pi h)$ , the stability boundary is well described by the following PGA threshold:

$$PGA = \frac{ag}{2} J_0^{-1} \left( \frac{aD_c}{bV_0T} \right) \quad (7)$$

where  $J_0^{-1}$  is the reciprocal of the modified Bessel function of the first kind and order 0. The PGA threshold predicted by this equation is of order 0.1 g. This asymptotic PGA threshold is represented by the vertical yellow lines on Figure 5. Theoretical analysis (Equation S16 in Supporting Information 1) shows that the asymptotic PGA threshold arises from the interference between upgoing and downgoing (reflected) waves at periods longer than  $\Delta T$ , which makes shear stress resemble an inertial response of the mass column overlying the slip surface. Note that inertial stresses are also assumed in rigid-block landslide models such as Newmark's method; our analysis shows that such approximation is justified only at sufficiently low frequencies.

At higher frequencies, the stability boundary features a diagonal envelope, which is well described by the following PGV threshold:

$$PGV \geq \frac{a\sigma_0 C_s}{2\mu} J_0^{-1} \left( \frac{aD_c}{bV_0T} \right) \quad (8)$$

This asymptotic behavior arises because, at periods shorter than  $\Delta T$ , the stresses on the slip surface are proportional to velocities (as in Equation 6). This high-frequency regime is not captured by rigid-block models. The yellow diagonal lines in Figure 5 correspond to this PGV threshold. Equations 7 and 8 can also be obtained from

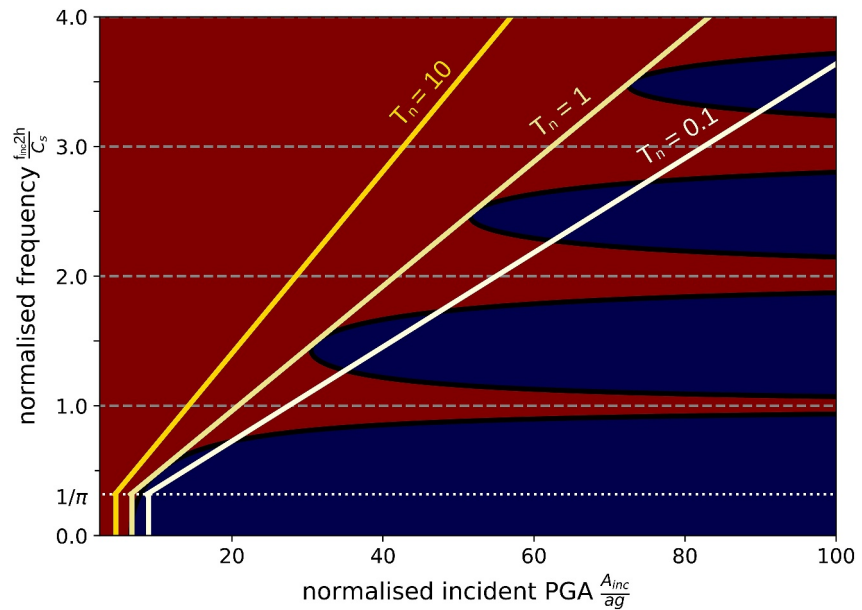


**Figure 5.** Non-dimensional landslide stability diagram as a function of incident wave frequency and amplitude, based on the theoretical analysis of Section 3.3. Frequency is normalized by the two-way travel time across the landslide thickness,  $\Delta T = 2h/C_s$ , and Peak Ground Acceleration by  $ag$  which is typically  $\approx 1\%g$ . The stability boundary (black curve separating stable slip in red from unstable slip in blue, predicted by the approximate Equation 48 in Text S2 in Supporting Information S1) is shown for an incident wave with normalized duration  $T_n = 4000 \times V_0 T/D_c$  set to 1. Asymptotic approximations (yellow curves; vertical for Equation 7 and diagonal for Equation 8) are shown for three normalized wave durations,  $T_n = 0.1, 1$ , and  $10$ .

the linear analysis, except for the  $I_0$  term, which is actually large. The analysis also predicts stable slip at the frequency  $1/\Delta T$  and its multiples (Figure 5), which is consistent with our simulation results (Figure 4b). These stable frequencies are those at which the shear stresses carried by the incident and reflected waves cancel each other. The rate-and-state parameter  $b$ , which controls the state evolution effect, and the sign of  $a - b$  do not significantly affect the predicted stability boundary; this is consistent with the simulation results in Figure 4.

#### 4. Discussion

Here we discuss implications and possible extensions of the model. From the previous theoretical results, we distill important implications on the effects of shaking duration, landslide thickness and pore fluid pressure on the seismic triggering of landslides. We then discuss extensions to more realistic incident waves, with oblique incidence, normal stress changes and broadband incident waves. Some extensions are straightforward, others require further work. Finally we evaluate the potential generalization and further opportunities of this method.

While we previously focused on the effects of frequency and amplitude of the incident wave, its duration  $T$  can also affect landslide triggering. Based on Equations 7 and 8 and noting that  $I_0(z) \sim \exp(z)/\sqrt{2\pi z}$  at large  $z$ , the effect of  $T$  on the stability boundary is relatively weak, quasi-logarithmic. This is illustrated in Figure 5 by the mild differences in the stability boundaries for  $T$  values spanning three orders of magnitude (yellow curves). More generally, the stability boundary depends mildly on the dimensionless number  $aD_c/bV_0T$ .

Considering  $\sigma_0$  is proportional to depth, Equation 8 predicts that high-frequency ground motions with a larger PGV can trigger deeper landslides, which can potentially mobilize larger masses. This can help explain observations that stronger ground motions trigger larger landslides (Valagussa et al., 2019). Interestingly, the low-frequency PGA threshold (Equation 7) does not depend on landslide thickness, although its maximum frequency of validity does.

In the presence of fluids along the slip surface, our model predicts enhanced triggered-landslide susceptibility. This is a natural result of the proportionality of frictional strength on effective normal stress. For a pore fluid pressure  $P$ , replacing  $\sigma_0$  by the effective normal stress  $\sigma_0 - P$  in the derivations in Supporting Information S1 results in PGA and PGV thresholds that are lower by the factor  $1 - P/\rho gh < 1$ .



Our theoretical results apply, with slight modifications, to obliquely incident SH waves. Given an incidence angle  $i$  relative to the slip surface normal direction, the results are valid upon accounting for the apparent wave speed along the direction normal to the slip surface,  $C_s/\cos(i)$ . The apparent wave impedance is  $\mu \cos(i)/C_s$  and the apparent two-way travel time  $\Delta T = 2h \cos(i)/C_s$ . The resulting low-frequency PGA threshold is given by Equation 7 divided by  $\cos(i)^2$ , and the high-frequency PGV threshold by Equation 8 divided by  $\cos(i)$ . Thus, the case of normal incidence ( $i = 0$ ) is the least stable, it has the lowest PGA and PGV thresholds for instability. This is consistent with the observation that landslides are triggered more often in slopes that are facing away from the earthquake hypocenter, for which wave incidence is closer to normal (Dunham et al., 2022; Meunier et al., 2008).

The results can also be extended to incident waves that induce normal stress changes  $\delta\sigma(t)$ , such as obliquely incident P-SV waves. This amounts to replacing the shear stresses induced by the incident and reflected waves  $\tau_{inc} + \tau_{ref}$ , by Coulomb stresses  $\tau_{inc} + \tau_{ref} - f_0\delta\sigma$ , where  $\delta\sigma$  includes the effects of incident and reflected waves and accounts for S/P conversions at the free surface. One could also account for other processes affecting the normal stress of the slip surface, such as poroelastic effects in saturated and non-saturated media (Delorey & Chen, 2022) or dilatancy (Iverson, 2005; Sakamoto & Tanaka, 2022). Depending on their relative phasing, shear and normal stress contributions to Coulomb stresses can interfere constructively or destructively, which can enhance or reduce the potential for landslide triggering (Brain et al., 2015).

Our model also applies to incident waves with more realistic, non-monochromatic waveform. In certain situations, we can use the derived amplitude thresholds even if the incident wave has a broad frequency content. The PGA criterion (Equation 7) applies if the incident acceleration spectrum is dominated by relatively low frequencies, namely if the maximum frequency set by attenuation ( $f_{max}$ ) is lower than  $1/\Delta T = C_s/2h$ . For typical values  $f_{max} = 10$  Hz,  $C_s$  of a few 100 m/s and  $h$  up to a few 10 m, the PGA criterion is appropriate. The PGV criterion (Equation 8) applies if the incident velocity spectrum is dominated by relatively high frequencies, specifically if both  $f_{max}$  and the corner frequency set by the earthquake source ( $f_c$ ) are higher than  $1/\Delta T$ . If  $1/\Delta T$  is low, say a few Hz, the PGV criterion can be appropriate for small magnitude earthquakes. In between these two end-member situations, when the incident frequency content straddles  $1/\Delta T$ , landslide stability according to our model can be assessed by the following procedure, based on the approximate non-linear analysis in Text S2 in Supporting Information S1. First, compute the stresses  $\tau_{inc} + \tau_{ref}$  induced on the slip surface by the input wavefield under the assumption of no slip, using Equations S2 and S3 in Supporting Information S1. Then, compute the function  $\dot{\phi}(t) = \exp\left(\frac{\tau_{inc} + \tau_{ref}}{a\sigma_0}\right)$  and integrate it. Finally, evaluate if the instability criterion  $\phi = aD_c/bV_0$  is achieved. This method requires the knowledge of rate-and-state parameters  $a$ ,  $b$ , and  $D_c$ , and the initial slip velocity  $V_0$ . However, the sensitivity of the stability condition to  $aD_c/bV_0$  is mild, as illustrated in the monochromatic case by Equations 7 and 8.

How general is the model? We expect the behavior to be qualitatively similar for other rheologies of the slip surface that comprise the following two basic ingredients: a non-linear viscosity and a slip-weakening mechanism. In rate-and-state friction, these ingredients are represented by the direct effect,  $a \log(V)$ , and the state evolution effect,  $b \log(\theta)$  (which tends to linear slip-weakening  $\approx -bD/D_c$  when well above steady-state). Different rheologies might involve different functional forms of these two ingredients (e.g., Puzrin et al., 2010), but we anticipate the qualitatively features of the model response to remain similar.

Additional opportunities to extend the model include: non-uniform slip, physical processes involving fluids on the slip surface (dilatancy, liquefaction or gas hydrates such as Handwerger et al. (2017)), delayed triggering or transient slip at longer timescale accounting for healing effects. Some of those topics can be addressed by variations of rate-and-state friction, such as a second state variable (Chau, 1999) or a modified state law to model the evolution of pore pressure.

Field observations indicate that many seismically triggered landslides are fresh rather than re-activated landslides (Keefer, 1984). It is conceivable that freshly triggered landslides start on a fully-buried incipient slip surface, formed earlier by shear localization. Our model applies to the triggered slip on such surface. In turn, this accelerated slip can drive the lateral growth of the slip surface, leading to a well-developed landslide. Modeling this coupled process deserves further work.

## 5. Conclusions

To advance the understanding of seismic triggering of landslides, we developed a model of slip initiation on pre-existing slip surfaces governed by laboratory-based rate-and-state friction in response to incident seismic waves. Through numerical simulations and theoretical analysis, we characterized how slope stability depends on friction properties, landslide thickness and incident wave properties (frequency content, duration, acceleration, or velocity amplitude). The model incorporates friction and wave propagation effects in a way that is not common in conventional triggered-landslide assessment approaches, and thus provides new insights. The slip surface weakens by steps with each incident wave cycle, and the frictional state variable tracks well this cyclic fatigue. Wave propagation effects introduce two regimes depending on frequency. At low frequencies relative to the two-way travel time across the landslide thickness, the stability criterion is well approximated by a threshold on the peak acceleration of the incident wave, as in the classical pseudo-static and Newmark analyses. At higher frequencies, a threshold on peak velocity provides an appropriate stability criterion. Our theoretical developments, validated by numerical simulations, can be used to apply the model to the evaluation of landslide stability under arbitrary input motions, without the need for simulations.

## Data Availability Statement

We used the open-source software SEM2DPACK, version 2.3.9 (Ampuero et al., 2024). Scripts for simulation and visualization, input files and sample output data from the simulations used in this article are available in the directory EXAMPLES/RS-landslides-lestrelin2024 of the SEM2DPACK software.

## Acknowledgments

HL was funded by a CEREMA PhD fellowship. JPA was supported by the French government through the UCAJEDI Investments in the Future project (ANR-15-IDEX-01) managed by the National Research Agency (ANR).

## References

- Agliardi, F., Scuderi, M. M., Fusi, N., & Collettini, C. (2020). Slow-to-fast transition of giant creeping rockslides modulated by undrained loading in basal shear zones. *Nature Communications*, 11(1), 1352. <https://doi.org/10.1038/s41467-020-15093-3>
- Ampuero, J. P., Oral, E., Currie, T., Weng, H., Lestrelin, H., Herreramena, M., et al. (2024). jpmuero/sem2dpack: Sem2dpack v2.3.9 [Software]. *Zenodo*. <https://doi.org/10.5281/zenodo.13821494>
- Ampuero, J. P., Vilotte, J., & Sánchez-Sesma, F. J. (2002). Nucleation of rupture under slip dependent friction law: Simple models of fault zone. *Journal of Geophysical Research*, 107(B12), 2324. <https://doi.org/10.1029/2001JB000452>
- Bird, J. F., & Bommer, J. J. (2004). Earthquake losses due to ground failure. *Engineering Geology*, 75(2), 147–179. <https://doi.org/10.1016/j.enggeo.2004.05.006>
- Brain, M. J., Rosser, N. J., Sutton, J., Snelling, K., Tunstall, N., & Petley, D. N. (2015). The effects of normal and shear stress wave phasing on coseismic landslide displacement. *Journal of Geophysical Research: Earth Surface*, 120(6), 1009–1022. <https://doi.org/10.1002/2014JF003417>
- Chau, K. T. (1995). Landslides modeled as bifurcations of creeping slopes with nonlinear friction law. *International Journal of Solids and Structures*, 32(23), 3451–3464. [https://doi.org/10.1016/0020-7683\(94\)00317-P](https://doi.org/10.1016/0020-7683(94)00317-P)
- Chau, K. T. (1999). Onset of natural terrain landslides modelled by linear stability analysis of creeping slopes with a two-state variable friction law. *International Journal for Numerical and Analytical Methods in Geomechanics*, 23(15), 1835–1855. [https://doi.org/10.1002/\(SICI\)1096-9853\(19991225\)23:15<1835::AID-NAG23>3.0.CO;2-2](https://doi.org/10.1002/(SICI)1096-9853(19991225)23:15<1835::AID-NAG23>3.0.CO;2-2)
- Chousianitis, K., Del Gaudio, V., Kalogeras, I., & Ganas, A. (2014). Predictive model of Arias intensity and Newmark displacement for regional scale evaluation of earthquake-induced landslide hazard in Greece. *Soil Dynamics and Earthquake Engineering*, 65, 11–29. <https://doi.org/10.1016/j.soildyn.2014.05.009>
- Clare, M., Lintern, D. G., Rosenberger, K., Hughes Clarke, J. E., Paull, C., Gwiazda, R., et al. (2020). Lessons learned from the monitoring of turbidity currents and guidance for future platform designs. In A. Georgiopolou, L. A. Amy, S. Benetti, J. D. Chaytor, M. A. Clare, D. Gamboa, et al. (Eds.), *Subaqueous mass movements and their consequences: Advances in process understanding, monitoring and hazard assessments* (Vol. 500, pp. 605–634). Geological Society of London. <https://doi.org/10.1144/SP500-2019-173>
- Dahal, A., Castro-Cruz, D. A., Tanyaş, H., Fadel, I., Mai, P. M., van der Meijde, M., et al. (2023). From ground motion simulations to landslide occurrence prediction. *Geomorphology*, 441, 108898. <https://doi.org/10.1016/j.geomorph.2023.108898>
- Delorey, A. A., & Chen, T. (2022). Behavior of tidally triggered earthquakes depends on fluid conditions. *Bulletin of the Seismological Society of America*, 112(6), 2890–2901. <https://doi.org/10.1785/0120220036>
- Dieterich, J. H. (1978). Time-dependent friction and the mechanics of stick-slip. In J. D. Byerlee & M. Wyss (Eds.), *Rock friction and earthquake prediction* (pp. 790–806). [https://doi.org/10.1007/978-3-0348-7182-2\\_15](https://doi.org/10.1007/978-3-0348-7182-2_15)
- Djukem, D. L. W., Fan, X., Braun, A., Chevalier, M.-L., Wang, X., Dai, L., et al. (2024). Traditional and modified Newmark displacement methods after the 2022 Ms 6.8 Luding earthquake (Eastern Tibetan plateau). *Landslides*, 21(4), 807–828. <https://doi.org/10.1007/s10346-023-02194-5>
- Dunham, A. M., Kiser, E., Kargel, J. S., Haritashya, U. K., Watson, C. S., Shugar, D. H., et al. (2022). Topographic control on ground motions and landslides from the 2015 Gorkha earthquake. *Geophysical Research Letters*, 49(10), e2022GL098582. <https://doi.org/10.1029/2022GL098582>
- Gatter, R., Clare, M. A., Kuhlmann, J., & Huhn, K. (2021). Characterisation of weak layers, physical controls on their global distribution and their role in submarine landslide formation. *Earth-Science Reviews*, 223, 103845. <https://doi.org/10.1016/j.earscirev.2021.103845>
- Goldfinger, C., Nelson, C. H., Morey, A. E., Johnson, J. E., Patton, J. R., Karabanov, E. B., et al. (2012). *Turbidite event history—Methods and implications for Holocene paleoseismicity of the Cascadia subduction zone* (Technical Report no. 1661-F). U.S. Geological Survey. <https://doi.org/10.3133/pp1661F>
- Gomberg, J. (2018). Cascadia Onshore-offshore site response, submarine sediment mobilization, and earthquake recurrence. *Journal of Geophysical Research: Solid Earth*, 123(2), 1381–1404. <https://doi.org/10.1002/2017JB014985>

- Gomberg, J., Bodin, P., Savage, W., & Jackson, M. E. (1995). Landslide faults and tectonic faults, analogs? The Slumgullion earthflow, Colorado. *Geology*, 23(1), 41–44. [https://doi.org/10.1130/0091-7613\(1995\)023\(0041:LFATFA\)72.3.CO;2](https://doi.org/10.1130/0091-7613(1995)023(0041:LFATFA)72.3.CO;2)
- Handwerger, A. L., Rempel, A. W., & Skarbek, R. M. (2017). Submarine landslides triggered by destabilization of high-saturation hydrate anomalies. *Geochemistry, Geophysics, Geosystems*, 18(7), 2429–2445. <https://doi.org/10.1002/2016GC006706>
- Handwerger, A. L., Rempel, A. W., Skarbek, R. M., Roering, J. J., & Hilley, G. E. (2016). Rate-weakening friction characterizes both slow sliding and catastrophic failure of landslides. *Proceedings of the National Academy of Sciences*, 113(37), 10281–10286. <https://doi.org/10.1073/pnas.1607009113>
- Helmstetter, A., Sornette, D., Anderssen, J., Gluzman, S., Grasso, J.-R., Guglielmi, Y., & Seve, G. (2001). Rate and state friction law as a model for landslide movements. In *AGU fall meeting abstracts*.
- Iverson, R. M. (2005). Regulation of landslide motion by dilatancy and pore pressure feedback. *Journal of Geophysical Research*, 110(F2), 341. <https://doi.org/10.1029/2004JF000268>
- Jibson, R. W. (2011). Methods for assessing the stability of slopes during earthquakes—A retrospective. *Engineering Geology*, 122(1), 43–50. <https://doi.org/10.1016/j.enggeo.2010.09.017>
- Kaneko, Y., Lapusta, N., & Ampuero, J.-P. (2008). Spectral element modeling of spontaneous earthquake rupture on rate and state faults: Effect of velocity-strengthening friction at shallow depths. *Journal of Geophysical Research*, 113(B9), B09316. <https://doi.org/10.1029/2007JB005553>
- Kang, X., Wang, S., Wu, W., & Xu, G. (2022). Residual state rate effects of shear-zone soil regulating slow-to-fast transition of catastrophic landslides. *Engineering Geology*, 304, 106692. <https://doi.org/10.1016/j.enggeo.2022.106692>
- Keefer, D. K. (1984). Landslides caused by earthquakes. *GSA Bulletin*, 95(4), 406–421. [https://doi.org/10.1130/0016-7606\(1984\)95\(406:LCBE\)2.0.CO;2](https://doi.org/10.1130/0016-7606(1984)95(406:LCBE)2.0.CO;2)
- Kelner, M., Migeon, S., Tric, E., Coubolex, F., Dano, A., Lebourg, T., & Taboada, A. (2016). Frequency and triggering of small-scale submarine landslides on decadal timescales: Analysis of 4D bathymetric data from the continental slope offshore Nice (France). *Marine Geology*, 379, 281–297. <https://doi.org/10.1016/j.margeo.2016.06.009>
- Kramer, S. L., & Smith, M. W. (1997). Modified Newmark model for seismic displacements of compliant slopes. *Journal of Geotechnical and Geoenvironmental Engineering*, 123(7), 635–644. [https://doi.org/10.1061/\(ASCE\)1090-0241\(1997\)123:7\(635\)](https://doi.org/10.1061/(ASCE)1090-0241(1997)123:7(635))
- Marone, C. (1998). Laboratory-derived friction laws and their application to seismic faulting. *Annual Review of Earth and Planetary Sciences*, 26(1), 643–696. <https://doi.org/10.1146/annurev.earth.26.1.643>
- Meunier, P., Hovius, N., & Haines, A. J. (2007). Regional patterns of earthquake-triggered landslides and their relation to ground motion. *Geophysical Research Letters*, 34(20), L20408. <https://doi.org/10.1029/2007GL031337>
- Meunier, P., Hovius, N., & Haines, J. A. (2008). Topographic site effects and the location of earthquake induced landslides. *Earth and Planetary Science Letters*, 275(3), 221–232. <https://doi.org/10.1016/j.epsl.2008.07.020>
- Newmark, N. M. (1965). Effects of earthquakes on Dams and embankments. *Géotechnique*, 15(2), 139–160. <https://doi.org/10.1680/geot.1965.15.2.139>
- Palmer, A. C., & Rice, J. R. (1973). The growth of slip surfaces in the progressive failure of over-consolidated clay. *Proceedings of the Royal Society of London. A. Mathematical and Physical Sciences*, 332(1591), 527–548.
- Paul, K., Bhattacharya, P., & Misra, S. (2024). Frictional control on accelerating creep during the slow-to-fast transition of rainfall-induced catastrophic landslides. *Journal of Geophysical Research: Earth Surface*, 129(1), e2023JF007213. <https://doi.org/10.1029/2023JF007213>
- Puzrin, A. M., Saurer, E., & Germanovich, L. N. (2010). A dynamic solution of the shear band propagation in submerged landslides. *Granular Matter*, 12(3), 253–265. <https://doi.org/10.1007/s10035-010-0177-8>
- Ruina, A. (1983). Slip instability and state variable friction laws. *Journal of Geophysical Research*, 88(B12), 10359–10370. <https://doi.org/10.1029/JB088iB12p10359>
- Sakamoto, R., & Tanaka, Y. (2022). Frictional and hydraulic properties of plate interfaces constrained by a tidal response model considering dilatancy/compaction. *Journal of Geophysical Research: Solid Earth*, 127(8), 384. <https://doi.org/10.1029/2022JB024112>
- Shanmugam, G., & Wang, Y. (2015). The landslide problem. *Journal of Palaeogeography*, 4(2), 109–166. <https://doi.org/10.3724/SP.J.1261.2015.00071>
- Skempton, A. W. (1985). Residual strength of clays in landslides, folded strata and the laboratory. *Géotechnique*, 35(1), 3–18. <https://doi.org/10.1680/geot.1985.35.1.3>
- Sultan, N., Cochonat, P., Canals, M., Cattaneo, A., Dennielou, B., Haflidason, H., et al. (2004). Triggering mechanisms of slope instability processes and sediment failures on continental margins: A geotechnical approach. *Marine Geology*, 213(1), 291–321. <https://doi.org/10.1016/j.margeo.2004.10.011>
- Tang, C., Zhu, J., Ding, J., Cui, X. F., Chen, L., & Zhang, J. S. (2011). Catastrophic debris flows triggered by a 14 August 2010 rainfall at the epicenter of the Wenchuan earthquake. *Landslides*, 8(4), 485–497. <https://doi.org/10.1007/s10346-011-0269-5>
- Valagussa, A., Marc, O., Frattini, P., & Crosta, G. B. (2019). Seismic and geological controls on earthquake-induced landslide size. *Earth and Planetary Science Letters*, 506, 268–281. <https://doi.org/10.1016/j.epsl.2018.11.005>
- Viesca, R. C., & Rice, J. R. (2012). Nucleation of slip-weakening rupture instability in landslides by localized increase of pore pressure. *Journal of Geophysical Research*, 117(B3), B03104. <https://doi.org/10.1029/2011JB008866>
- Wang, G., Suemine, A., Zhang, F., Hata, Y., Fukuoka, H., & Kamai, T. (2014). Some fluidized landslides triggered by the 2011 Tohoku earthquake (Mw 9.0), Japan. *Geomorphology*, 208, 11–21. <https://doi.org/10.1016/j.geomorph.2013.11.009>

## References From the Supporting Information

- Ader, T. J., Lapusta, N., Avouac, J.-P., & Ampuero, J.-P. (2014). Response of rate-and-state seismogenic faults to harmonic shear-stress perturbations. *Geophysical Journal International*, 198(1), 385–413. <https://doi.org/10.1093/gji/ggu144>
- Rice, J. R. (1993). Spatio-temporal complexity of slip on a fault. *Journal of Geophysical Research*, 98(B6), 9885–9907. <https://doi.org/10.1029/93JB00191>